DOI:10.1002/ejic.201402529

Chemodosimetric Detection of the Acetate Anion by Using the Template Reaction Method via a Fluorescence “Turn-Off” Signal

Sudhanshu Das,[a] Sankar Jana,[a] Prateeti Chakraborty,[a] Ria Sanyal,[a] Dilip Kumar Maiti,[a] Nikhil Guchhait,[a] Ennio Zangrando,*[b] and Debasis Das*[a]

Keywords: Chemodosimeter / Chemosensors / Fluorescence / Anions / Copper

The compartmental ligand 2,6-bis[2-(*N*-ethyl)thiopheneiminomethyl]-4-chlorophenol (HL) undergoes $Cu(ClO_4)_2$ induced partial hydrolysis to yield a monoamine ligand 4-chloro-2-formyl-6-[2-(thiophen-2-yl)ethyliminomethyl]-phenol (HL′). On further reaction with $Cu(ClO_4)_2$, HL′ produces a dinuclear complex, $[Cu_2(L')_2(ClO_4)_2]$ (**2**), which has been characterized in solution by UV/Vis, ATR, NMR, and ESI-MS spectral techniques and in the solid state by X-ray single-crystal structure analysis. The in situ generated **2** is highly fluorescent. On reaction with sodium acetate it transforms to a fluorescence inactive tetranuclear species, $[Cu_4(L)_2(OAc)_4(O)]$ (**3**), and thereby acts as an excellent chemodosimeter for selective detection of the acetate anion via fluorescence “turn-off” signalling. The direct reaction of HL and copper(II) acetate dihydrate yielded another fluorescence inactive tetranuclear species, $[Cu_4(L)_2(OAc)_4(O)]$ (**1**), which is a diastereoisomer of **3** as is evident from X-ray single-crystal structural analyses.

Introduction

Selective detection of inorganic and biotic anions at a very low concentration by simple, inexpensive and quick methods is a great challenge to the chemists as well as biologists because these anions play fundamental roles in the environment, biological processes, medicine, catalysis, and molecular assembly.[1–4] Considerable efforts have been made to design the appropriate detecting systems, which are mainly chemosensors based on noncovalent interactions including hydrogen bonding, π–π, donor–acceptor, electrostatic, hydrophobic, hydrophilic, and coordination-based interactions.[5–11] In these approaches, the change in fluorescence or color is reversible in principle. A very different approach, now popularly known as the chemodosimetric approach was first introduced in 1992 by Chae and Czarnik.[12–19] This approach involves the use of anion-induced reactions where the signaling process is coupled to an irreversible chemical reaction. The chemodosimetric approach is rather new and looks more promising than the chemosensor method because of its advantage of the selective reactivity that a certain anion may display over others. Following the coordination of the binding site to a certain anion, some spectroscopic characteristics (color, fluorescence, etc.) change. Among these, fluorescence signal detection is particularly attractive because of its simplicity and high sensitivity. Acetate, which is a crucial component in numerous metabolic processes,[20,21] is the anion in which we are interested in. It is worth mentioning that in designing chemosensor fluorescence quenching is a well-established technique to detect target molecules.[22–27] In this report, we have demonstrated for the first time a chemodosimetric approach for the selective detection of acetate anion by exploring a metallo–ligand i.e. a dinuclear copper(II)-Schiff-base complex, $[Cu_2(L')_2(ClO_4)_2]$ (**2**) {where HL′ = 4-chloro-2-formyl-6-[2-(thiophen-2-yl)ethyliminomethyl] phenol} as a chemodosimeter formed in situ by the reaction of copper(II) perchlorate with the ligand 2,6-bis[2-(*N*-ethyl) thiopheneiminomethyl]-4-chlorophenol (HL). The ligand HL′ is obtained in situ by copper(II) percholarate induced partial hydrolysis of the ligand (HL). The in situ generated complex **2** is highly fluorescent, which on reaction with sodium acetate undergoes an easy transformation to a fluorescence-inactive tetranuclear copper(II) species $[Cu_4(L)_2(OAc)_4(O)]$ (**3**). Thus, the complex **2** acts as an effective chemodosimeter for acetate anion via fluorescence “turn-off” signaling. The selectivity of **2** has been explored on the basis of fluorescence quenching of the metallo–ligand in the presence of different anions. Here it is worth noting that HL on reaction with copper(II) acetate yielded another tetranuclear species, $[Cu_4(L)_2(OAc)_4(O)]$ (**1**), which

---

[a] Department of Chemistry, University of Calcutta,
92 A. P. C. Road, Kolkata 700009, India
E-mail: dasdebasis2001@yahoo.com
[b] Dipartimento di Scienze Chimiche e Farmaceutiche, University of Trieste,
Via L. Giorgieri 1, 34127, Trieste, Italy

Supporting information for this article is available on the WWW under http://dx.doi.org/10.1002/ejic.201402529.

is a diastereoisomer of **3** as is evident from X-ray single-crystal structural analyses.

Results and Discussion

In situ Generation of the Chemodosimeter 2 in an Acetonitrile Medium

Scheme 1 summarizes the reactions we have performed on the way to developing the system for selective detection of acetate anion by the chemodosimetric approach. The treatment of $Cu(OAc)_2\cdot H_2O$ with a phenol based "end-off" compartmental ligand HL, 2,6-bis[2-(*N*-ethyl)thiophene-iminomethyl]-4-chlorophenol, in acetonitrile, yielded the tetranuclear Cu^{II} complex **1** with four acetato moieties as bridging ligands. Then it was planned to synthesize the same complex with the stepwise addition of $Cu(ClO_4)_2$ to an acetonitrilic solution of HL followed by sodium acetate. The interaction between copper(II) perchlorate and the ligand (HL) produces a dinuclear copper(II) complex (**2**) having a partially hydrolyzed monoamine ligand (HL′) {where HL′ = 4-chloro-2-formyl-6-[2-(thiophen-2-yl)ethyliminomethyl]phenol}. In situ addition of sodium acetate immediately converts this dinuclear species to the tetranuclear copper(II) complex (**3**). The dinuclear copper(II) complex has been considered as a chemodosimeter for the selective detection of the acetate anion in an acetonitrile solvent. Generation of the dinuclear copper(II) complex and its conversion to the tetranuclear species have extensively been monitored and characterized by means of UV/Vis, ATR, NMR, and ESI-MS spectral techniques.

Spectroscopic Characterization of the Dinuclear Copper Chemodosimeter 2 Formed in situ

Spectrophotometric Study

Ligand HL (100 µM) exhibits band maxima at 450 and 350 nm in acetonitrile. The changes in the UV/Vis spectra upon progressive addition of copper(II) perchlorate (0 to 100 µM) are depicted in Figure 1. At a very low concentration of copper(II) perchlorate (0 to 20 µM, Figure 1, a) the

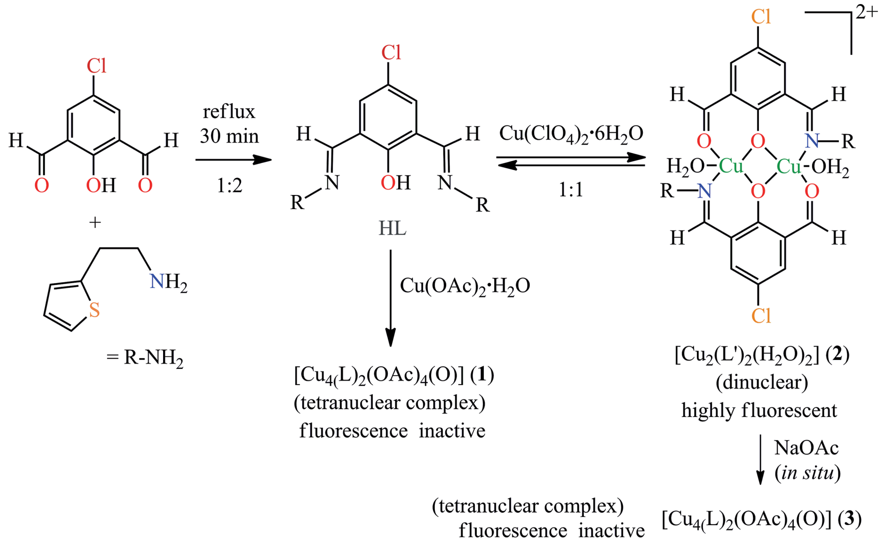

Scheme 1. Reaction scheme for the formation of **3**.

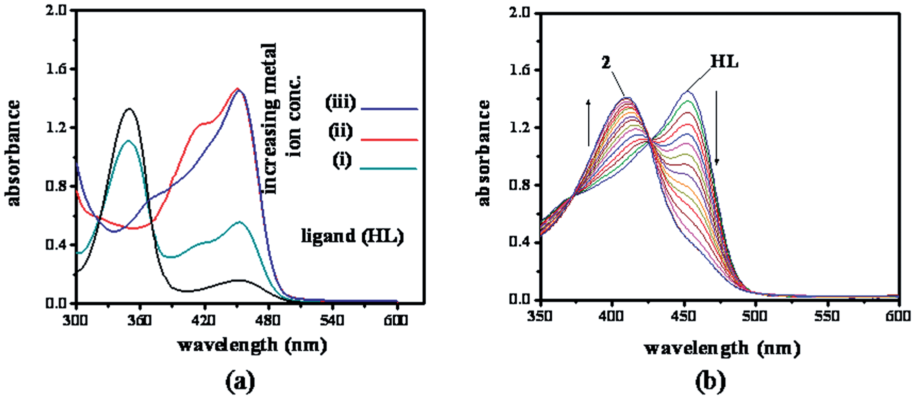

Figure 1. (a) the initial increment of the band at 450 nm at a very low concentration of copper perchlorate (from 0 to 20 µM); (b) formation of **2** upon addition of different concentrations of copper perchlorate (from 20 to 100 µM) to the ligand (100 µM) in acetonitrile.

band at 455 nm (π–π* transition) is observed to increase with a concomitant decrease in the band at 355 nm (n–π*). This may be ascribed to deprotonation of the phenolic –OH group of the ligand. Figure 1 (b) shows a decrease in the band at 450 nm with a concomitant increase of a new band centered at ca. 411 nm on further addition of copper(II) perchlorate (ligand-to-metal charge-transfer transition band). However, on excess addition of $Cu(ClO_4)_2$ the band at 411 nm does not increase significantly. The species corresponding to the band at 411 nm was labeled as **2**.

In the very next experiment progressive dropwise addition of sodium acetate to the solution of **2** was carried out and the corresponding spectral changes have been depicted in Figure 2. Successive addition of sodium acetate causes the gradual decrease of the band at 411 nm with a concomitant increment of a band centered at ca. 373 nm (complex **3**), a band maxima very close to the band maxima exhibited by complex **1** in acetonitrile (S1, Supporting Information).

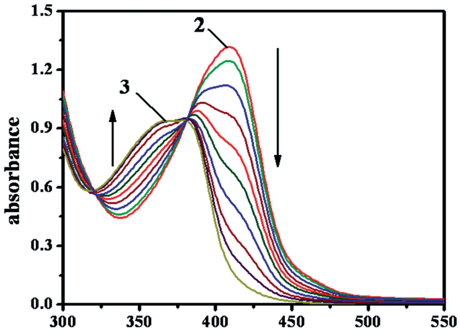

Figure 2. UV/Vis spectrophotometric titration of **2** in acetonitrile upon addition of an increasing concentration of acetate anion (0–200 μM) as tetrabutylammonium salt.

ATR Spectral Study

In order to characterize the species **2**, which appears as the key intermediate, we have performed an ATR titration (Figure 3). The ligand HL exhibits a band at 1638 cm^{-1} characteristic of C=N stretching. The ATR spectrum obtained after fresh mixing of $Cu(ClO_4)_2$ with HL exhibits stretching frequencies at 1665 and 1628 cm^{-1} suggesting the presence of C=O and C=N moieties, respectively, in the ligand present in complex **2**. The band at 1665 cm^{-1} shows a gradual diminish in intensity upon progressive addition of sodium acetate, an indication of the transformation of C=O to C=N.

NMR Spectral Study

In order to confirm the appearance of the free formyl group in species **2**, ^{1}H NMR titration has been performed by using $Zn(ClO_4)_2$ instead of $Cu(ClO_4)_2$ in [D$_6$]-DMSO solvent (Figure 4). As we failed several times to collect a conclusive spectrum using copper perchlorate, which is paramagnetic in nature, the titration experiment was conducted by using zinc perchlorate. The intension was to make sure of the appearance of the formyl group although it is important to note that the coordination environment of Zn^{II} may not be identical with that of Cu^{II}. The proton signal at 8.5 ppm observed in the ^{1}H NMR spectrum of HL is a clear indication of the presence of an imine group as expected. Interestingly, a new signal at δ = 10.22 ppm appeared in the spectrum after addition of $Zn(ClO_4)_2$ to the solution containing the ligand (not exceeding a 1:2 molar ratio of HL to the metal perchlorate) along with a signal at 8.5 ppm indicating the formation of a monoimine ligand comprising both the C=O and C=N moieties, which is supposed to be involved in the formation of the copper(II) spe-

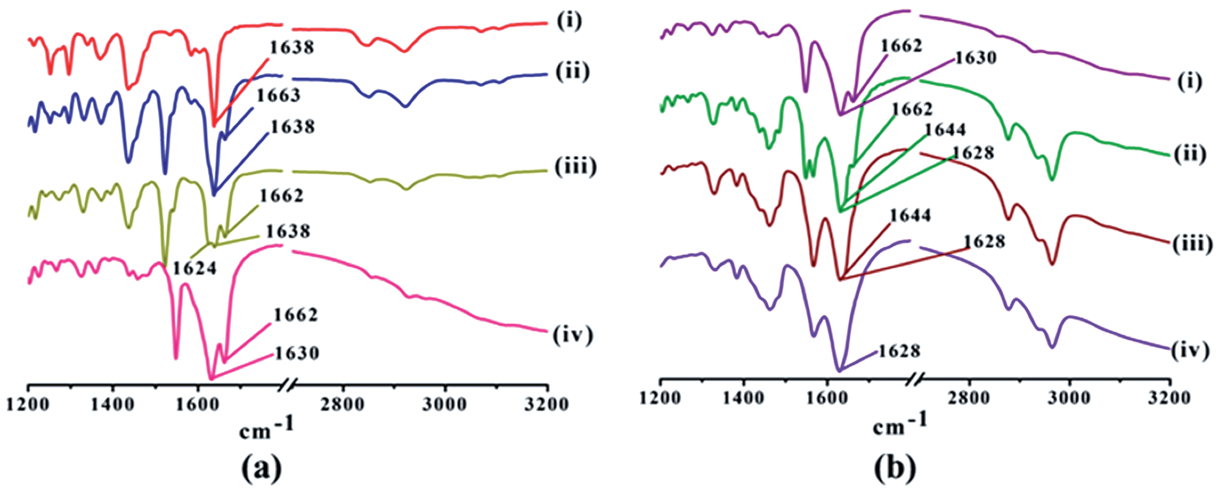

Figure 3. ATR titration of (a) ligand HL (3.0×10^{-3} mM) upon addition of various concentrations of copper perchlorate (0–3.0 mM, i–iv) in acetonitrile solvent and (b) solution mixture (chemodosimeter **2**) upon addition of various concentrations of acetate anion (0–7.5 mM, i–iv) in acetonitrile solvent. Acetate anion was added as a tetrabutylammonium salt.

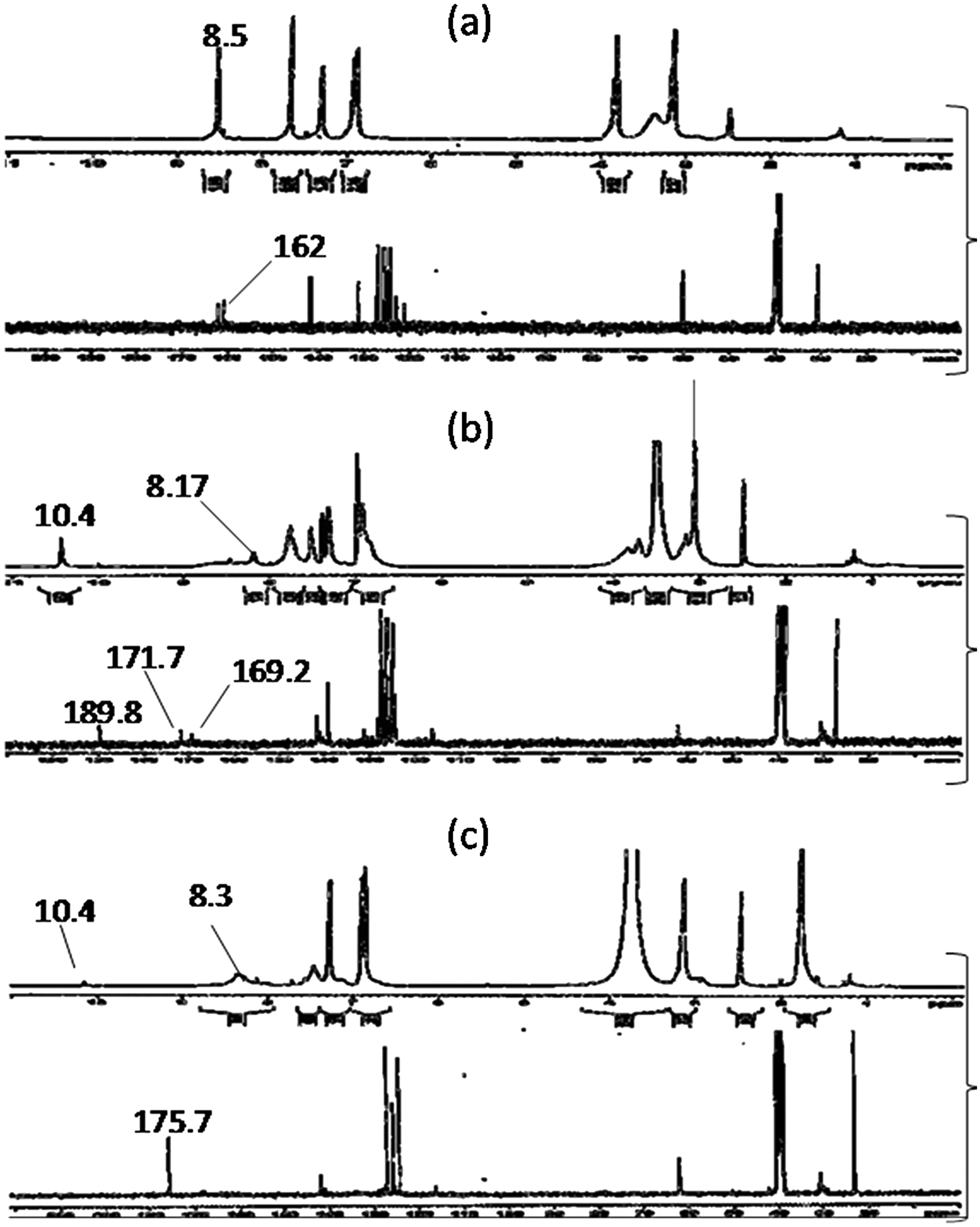

Figure 4. ^{1}H and ^{13}C NMR spectra of different species that appeared in solution during the formation of complex **3**. (a) Ligand (HL) in [D$_6$]DMSO; (b) spectra of a mixture of HL and $Zn(ClO_4)_2$ after 40 min and (c) spectra of a mixture of HL and $Zn(ClO_4)_2$ after 1 h in the presence of excess NaOAc.

cies (**2**). Once the complexation between zinc perchlorate and ligand is over (confirmed by monitoring the signal intensity at δ = 10.22 ppm) solid sodium acetate was added to the solution in the tube and the signals at 8.5 and 10.22 ppm were monitored again by taking successive scans with time. The signal at δ = 10.22 ppm was found to disappear with the concomitant increase in the signal intensity at 8.5 ppm. The ^{1}H NMR titration clearly confirms that formation of the intermediate occurs through metal(II) catalyzed hydrolysis of ligand HL and subsequent metalation of partially hydrolyzed ligand HL′, when we followed a stepwise reaction process.

ESI-MS Spectral Study

An ESI-MS spectrum of chemodosimeter **2** was taken after 45 min of equilibration of a reaction mixture of the ligand and copper perchlorate (shown in Figure 5). A prominent peak observed at m/z = 403.0855 amu corresponds to a dipositive copper species $[C_{28}H_{22}N_2O_4Cl_2S_2Cu_2 + 4Na]^{2+}$ (M_r = 801 g mol^{-1}). Simulation spectra corroborate well with the peak m/z = 403.0855 amu (calculated m/z = 400.92, 402.92, and 404.92 amu), which clearly indicates that a dinuclear copper(II) complex is formed by the reaction between ligand HL and copper perchlorate.

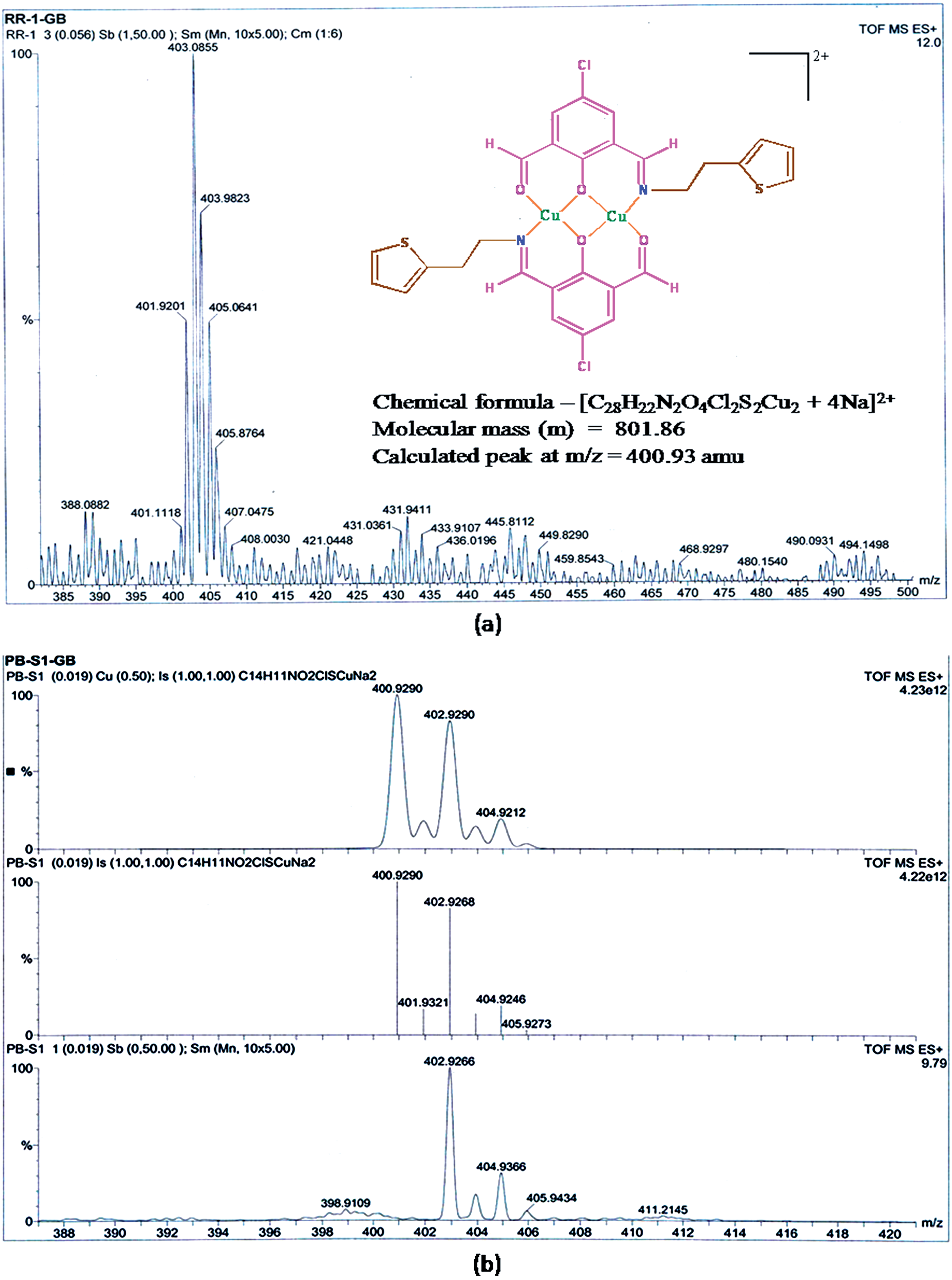

Figure 5. (a) ESI-MS and (b) simulation spectra of chemodosimeter **2** formed in situ by the reaction between copper(II) perchlorate and ligand HL in an acetonitrile solvent.

Structural Description of Complexes 1, 2, and 3

The X-ray structural characterization of compound **2** reveals that it is comprised of a dinuclear complex cation and perchlorate anions with the chemical formula $[Cu_2(L')_2(ClO_4)_2]$. The complex is built by two unsymmetrical tridentate ligands chelating the metal ions and forming a phenoxido-bridged Cu^{II} dimer in a centrosymmetrical fashion. The perchlorate anions located on both sides of the phenolate plane complete the coordination sphere of the metals. An ORTEP view with atom labeling scheme of the independent part is shown in Figure 6, and a selection of bond lengths and angles is given in Table 1. The symmetry related copper ions exhibit an octahedral coordination sphere, with two phenoxido-bridged oxygen atoms, an imine nitrogen donor, and carbonyl oxygen atom located in the basal plane, while two perchlorate oxygen atoms occupy the axial positions with longer bond lengths. All the Cu–N and Cu–O bond lengths are comparable varying within the range 1.933(3)–1.941(3) Å, while the axial distances are significantly longer because of the Jahn–Teller effect [the Cu–$OClO_3$ bond lengths are 2.501(10) and 2.527(4) Å]. The bridging bond angle Cu–O1–Cu′ is 101.00(13)°, leading to an intermetallic separation of 2.989(1) Å. The thiophene moieties, which are conformationally disordered, point away from the metal center.

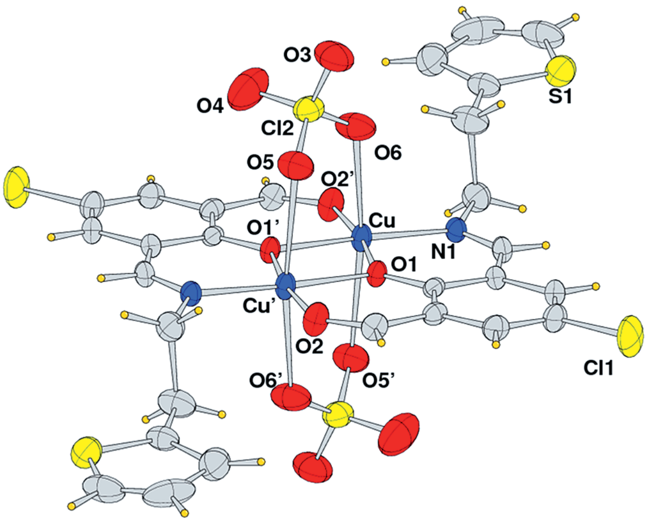

Figure 6. Molecular structure (ORTEP drawing, ellipsoids at 30% probability) of $[Cu_2(L')_2(ClO_4)_2]$ (**2**) with atom labeling scheme of the hetero atoms.

Table 1. Coordination bond lengths [Å] and angles [°] for complex **2**.

Cu–O(1)	1.933(3)	Cu–N(1)	1.936(4)
Cu–O(1)#1	1.940(3)	Cu–O(5)#1	2.501(4)
Cu–O(2)#1	1.941(3)	Cu–O(6)	2.527(4)
Cu–Cu#1	2.9888(12)		
O(1)–Cu–O(1)#1	78.99(13)	O(1)#1–Cu–O(5)#1	83.51(14)
O(1)–Cu–O(2)#1	170.68(14)	O(1)#1–Cu–O(6)	85.14(16)
O(1)–Cu–N(1)	93.99(14)	O(2)#1–Cu–O(5)#1	93.65(15)
O(1)#1–Cu–O(2)#1	91.73(14)	O(2)#1–Cu–O(6)	96.26(18)
O(1)#1–Cu–N(1)	172.98(14)	N(1)–Cu–O(5)#1	95.81(14)
O(2)#1–Cu–N(1)	95.28(15)	N(1)–Cu–O(6)	94.28(17)
O(1)–Cu–O(5)#1	84.43(15)	O(6)–Cu–O(5)#1	165.14(16)
O(1)–Cu–O(6)	84.02(18)	Cu–O(1)–Cu#1	101.00(13)

Symmetry code: #1 $-x + 2, -y + 2, -z$

Complexes **1** and **3** are tetranuclear copper(II) species with the chemical formula $[Cu_4(L)_2(OAc)_4(O)]$ and their molecular structures are shown in Figure 7. These complexes are best described as built up of two Cu_2L units con-

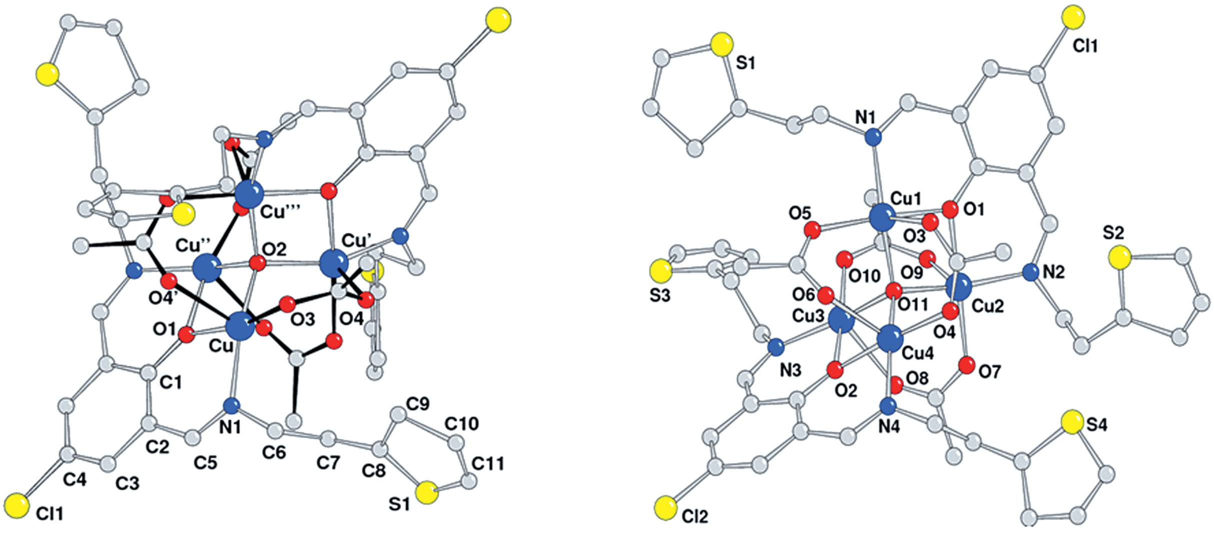

1 **3**

Figure 7. Molecular structures of **1** and **3**, with the atom labeling scheme. Complex **3** is located on a crystallographic fourfold improper axis.

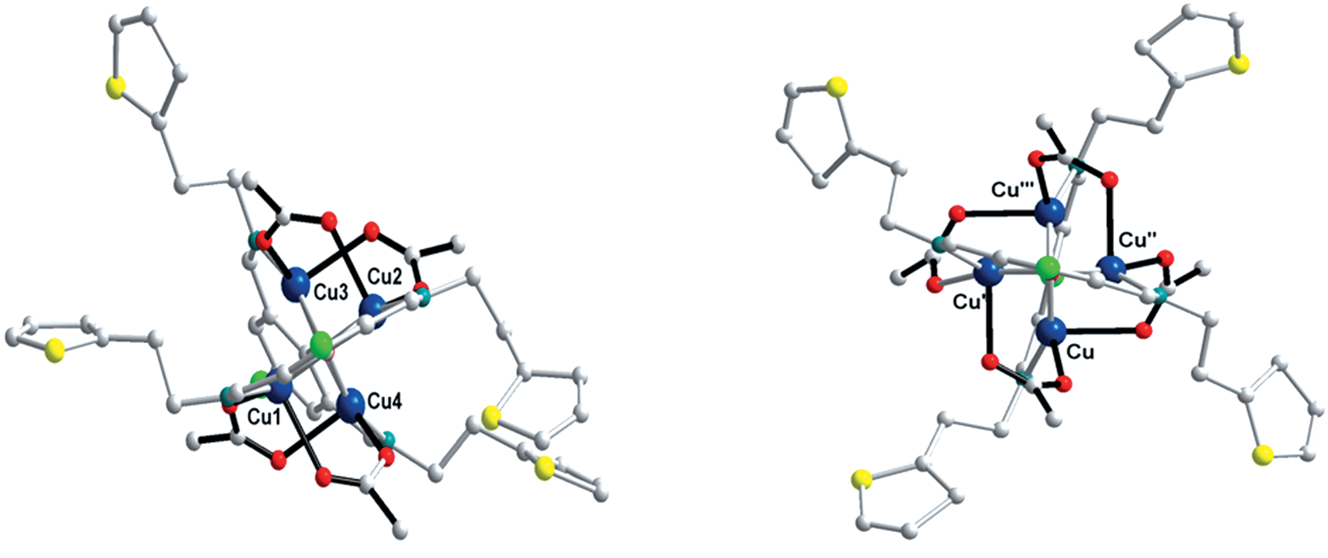

1 **3**

Figure 8. A view down the phenolato oxygen atoms showing the different coordination modes of acetate anions and the different thiophene arrangement in complex **1** and **3** (fourfold symmetry).

nected through a central μ_4-bridging oxido ligand and by four bridging acetate anions. All the Cu^{II} metal ions present a distorted square-planar pyramidal coordination geometry with trigonal τ index varying between 0.04 and 0.22. The basal bond lengths fall in a range from 1.910(5) to 1.999(5) Å, and among these the Cu–O(oxido) distances show the lower values, indicating, as expected, stronger bonds. In all cases a carboxylate oxygen occupies the apical position at a significantly longer distance [range 2.275(7)–2.340(6) Å]. The metals bridged by each ligand, L, are separated by 2.9892(14) and 2.9854(15) Å in **1** and by 3.0217(10) Å in **3**, while the Cu–Cu tetrahedron edges bridged by acetate anions are slightly longer, within 3.132(1)–3.247(1) Å in **1** and 3.162(8) Å in **3**. The two Cu_2L phenolato fragments are oriented almost perpendicular to each other and the dihedral angles between the mean planes are 73.6 and 90.0° in **1** and **3**, respectively. Complex **3** being located on a crystallographic fourfold improper axis, shows a high symmetry with the thiophene groups perfectly settled around the tetranuclear metal core. However, neglecting the arrangement of the thiophene groups, complexes **1** and **3** are diastereomers because of the different coordination mode exhibited by the bridging carboxylates, as shown in

Table 2. Coordination bond lengths [Å] and angles [°] for complex **1**.

Cu(1)–O(1)	1.999(5)	Cu(3)–O(2)	1.987(6)
Cu(1)–O(3)	2.315(6)	Cu(3)–O(8)	2.340(6)
Cu(1)–O(5)	1.946(6)	Cu(3)–O(10)	1.923(6)
Cu(1)–O(11)	1.913(5)	Cu(3)–O(11)	1.924(5)
Cu(1)–N(1)	1.984(7)	Cu(3)–N(3)	1.989(7)
Cu(2)–O(1)	1.980(5)	Cu(4)–O(2)	1.978(6)
Cu(2)–O(7)	1.937(6)	Cu(4)–O(4)	1.941(6)
Cu(2)–O(9)	2.309(6)	Cu(4)–O(6)	2.275(7)
Cu(2)–O(11)	1.912(5)	Cu(4)–O(11)	1.910(5)
Cu(2)–N(2)	1.987(6)	Cu(4)–N(4)	1.978(7)
Cu(1)–Cu(2)	2.9892(14)	Cu(3)–Cu(4)	2.9854(15)
O(1)–Cu(1)–O(3)	84.6(2)	O(2)–Cu(3)–O(8)	86.4(3)
O(1)–Cu(1)–O(5)	169.2(3)	O(2)–Cu(3)–O(10)	168.7(3)
O(1)–Cu(1)–O(11)	79.7(2)	O(2)–Cu(3)–O(11)	79.7(2)
O(1)–Cu(1)–N(1)	89.4(2)	O(2)–Cu(3)–N(3)	90.2(3)
O(3)–Cu(1)–O(5)	105.2(3)	O(8)–Cu(3)–O(10)	103.7(3)
O(3)–Cu(1)–O(11)	96.1(2)	O(8)–Cu(3)–O(11)	93.6(2)
O(3)–Cu(1)–N(1)	99.5(2)	O(8)–Cu(3)–N(3)	97.4(3)
O(5)–Cu(1)–O(11)	94.4(2)	O(10)–Cu(3)–O(11)	94.6(2)
O(5)–Cu(1)–N(1)	93.5(3)	O(10)–Cu(3)–N(3)	93.3(3)
O(11)–Cu(1)–N(1)	160.0(3)	O(11)–Cu(3)–N(3)	164.6(3)
τ Cu(1)	0.153	τ Cu(3)	0.068
O(1)–Cu(2)–O(7)	167.6(3)	O(2)–Cu(4)–O(4)	172.4(3)
O(1)–Cu(2)–O(9)	85.1(2)	O(2)–Cu(4)–O(6)	84.8(3)
O(1)–Cu(2)–O(11)	80.1(2)	O(2)–Cu(4)–O(11)	80.3(2)
O(1)–Cu(2)–N(2)	90.1(2)	O(2)–Cu(4)–N(4)	87.9(3)
O(7)–Cu(2)–O(9)	106.5(3)	O(4)–Cu(4)–O(6)	102.5(3)
O(7)–Cu(2)–O(11)	94.0(2)	O(4)–Cu(4)–O(11)	96.4(2)
O(7)–Cu(2)–N(2)	93.4(3)	O(4)–Cu(4)–N(4)	93.5(3)
O(11)–Cu(2)–O(9)	96.5(2)	O(6)–Cu(4)–N(4)	96.0(3)
O(11)–Cu(2)–N(2)	165.2(2)	O(6)–Cu(4)–O(11)	97.7(2)
O(9)–Cu(2)–N(2)	93.7(2)	O(11)–Cu(4)–N(4)	160.9(3)
τ Cu(2)	0.040	τ Cu(4)	0.192

Table 3. Coordination bond lengths [Å] and angles [°] for complex **3**.

Cu–O(1)	1.980(2)	Cu–O(3)	1.962(3)
Cu–O(2)	1.9082(5)	Cu–O(4)′	2.300(3)
Cu–N(1)	1.956(3)	Cu–Cu′′	3.0217(10)
O(2)–Cu–N(1)	156.28(10)	O(3)–Cu–O(1)	169.51(10)
O(2)–Cu–O(3)	96.10(8)	O(2)–Cu–O(4)′	93.74(8)
N(1)–Cu–O(3)	98.64(13)	N(1)–Cu–O(4)′	105.74(12)
O(2)–Cu–O(1)	77.93(8)	O(3)–Cu–O(4)′	85.91(12)
N(1)–Cu–O(1)	89.88(12)	O(1)–Cu–O(4)′	85.89(8)

Symmetry codes (′) at $-y + 3/4$, $x - 1/4$, $-z + 3/4$; (′′) at $-x + 1$, $-y + 1/2$, z

Figure 8. As reported earlier[28] by us, the configuration in **3** appears as the thermodynamic more stable one with respect to the diastereomer where pairs of acetate anions connect the same copper ions as in **1** (see Tables 2 and 3).

Fluorescence Spectra and Quantum Yield of Chemodosimeter 2

Photoluminescence studies of **1** and **3** in acetonitrilic solution reveals that both are non-fluorescent, in contrast to **2**, which was observed to be highly fluorescent (λ_{ex} = 410 nm and λ_{emi} = 488 nm with quantum yield Φ_f = 0.44). The fluorescence quantum yield of the chemodosimeter **2** in acetonitrile solvent was measured relative to anthracene in ethanol (Φ_f = 0.27) as secondary standard and calculated on the basis of Equation (1).[29]

$$\Phi_f = \Phi_f^0 \frac{n^2 A^0 \int I_f(\lambda_f) d\lambda_f}{n_0^2 A \int I_f^0(\lambda_f) d\lambda_f} \qquad (1)$$

Where n_0 and n are the refractive indices of the solvents, A^0 and A are the absorbances, Φ^0_f and Φ_f are the quantum yields and the integrals denote the area of the fluorescence bands for the standard and the sample, respectively.

Acetate Anion Selectivity of Chemodosimeter 2 in Acetonitrile

In order to establish the selectivity of chemodosimeter **2** we performed in situ fluorimetric titration by addition of various anions (in the form of tetrabutylammonium salt) to a fresh solution of **2** prepared in acetonitrile by the reaction between copper(II) perchlorate and the ligand (HL). Anions like phosphate, sulfate, nitrate, and iodide were observed to enhance the fluorescence intensity at varied degrees, whereas fluoride, chloride, bromide, and hydroxide were nearly non-effective (see Figure 9). Interestingly, the acetate anion had a quenching effect provided that **2** is a chemodosimetric probe for selective recognition of acetate anion via fluorescence "turn-off" signaling.

A fluorescence titration of **2** at variable concentrations of acetate anions revealed that 100% quenching occurs even at 10 µM of acetate concentration. Figure 10 shows the photographs of fluorescence changes of **2** in the presence of various anions (25 µM each) excited at 365 nm using a UV lamp as the visual impact indicating the effectiveness of the chemodosimeter **2** for the detection of acetate anions.

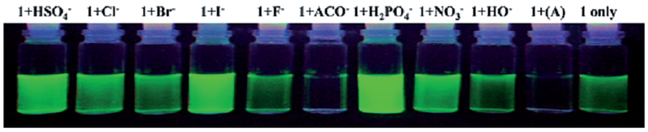

Figure 10. Photographs of fluorescence changes of **2** (3.12×10^{-5} M in acetonitrile medium) in the presence of various anions (25 µM each) excited at 365 nm using a UV lamp. Anions were added in the form of tetrabutylammonium salts ([A] represents a mixture of acetate and other anions at equal concentration).

Time Resolved Measurements and Fluorescence Lifetime

In order to know the exact origin of the quenching mechanism (dynamic or static) of chemodosimeter **2** in the presence of acetate anions, time resolved measurements have also been carried out. The chemodosimeter shows single exponential decay (Figure 11) with a fluorescence lifetime of 5.320 ns. On gradual addition of acetate ion the decay remains a single exponential with an unaltered lifetime (see Table 4). The Stern–Volmer plot of lifetime ratio against acetate anion concentration [see Equation (2) given below] has been found to be linear. The result demonstrates that quenching occurs via a static quenching ($\tau_0 = \tau$) mechanism[30–32] through the formation of a ground-state tetranuclear complex.

$$\tau_0/\tau = 1 + k_q \tau [Q] \qquad (2)$$

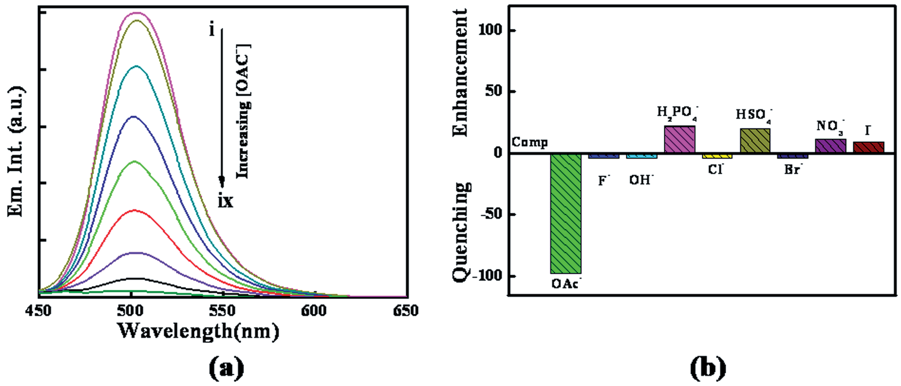

Figure 9. (a) Fluorescence spectra of **2** (2.5 µM) in acetonitrile solution upon addition of various concentrations of the acetate anion (0–10 µM) as tetrabutylammonium salt. (b) Effect of various anions in the fluorescence intensity of **2**.

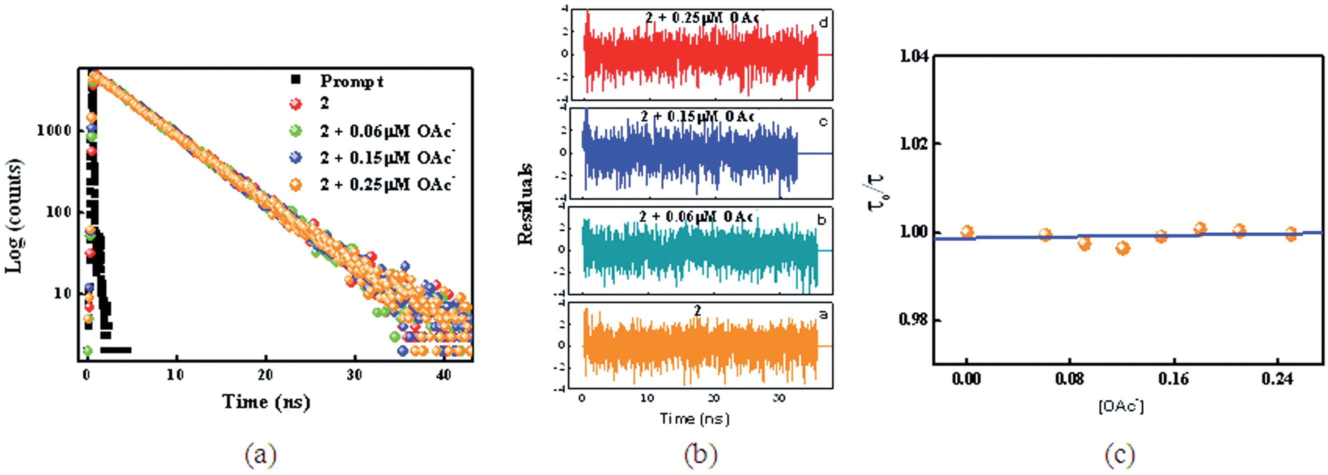

Figure 11. (a) Time-resolved decay profile, (b) corresponding residuals (1→4) and (c) Stern–Volmer plot of chemodosimeter **2** with increase in acetate anion concentration monitoring at emission maxima (411 nm) in acetonitrile solvent at room temperature.

Table 4. Life time data obtained from titration of **2** with the acetate anion.

Entry	τ [ns]	χ^2
2 + 0.0 μM AcO⁻	5.320	1.105
2 + 0.06 μM AcO⁻	5.317	1.022
2 + 0.09 μM AcO⁻	5.307	1.109
2 + 0.12 μM AcO⁻	5.301	1.028
2 + 0.15 μM AcO⁻	5.315	1.033
2 + 0.18 μM AcO⁻	5.324	1.077
2 + 0.21 μM AcO⁻	5.322	1.101
2 + 0.25 μM AcO⁻	5.318	1.096

Conclusions

The treatment of copper(II) acetate with HL produces a tetranuclear species $[Cu_4(L)_2(OAc)_4(O)]$ (**1**), which is fluorescence inactive. Interestingly, the ligand HL, in the presence of copper(II) perchlorate, undergoes partial hydrolysis and the monoamine ligand HL′ thus formed on reaction with copper(II) perchlorate generates a dinuclear Cu^{II} species (**2**), which is highly fluorescent. The structure of **2** in solution as well as in the solid state has been authenticated by several spectroscopic means. In situ addition of sodium acetate to the solution of **2** ultimately produces a new tetranuclear complex, $[Cu_4(L)_2(OAc)_4(O)]$ (**3**), which is a diastereoisomer of **1** as is evident from X-ray structure analyses. However, complex **3** is also non-fluorescent like **1**. Extensive investigation on the effect of several anions on fluorescence behavior of in situ generated **2** establishes undisputedly that species **2** is a chemodosimeter for selective detection of acetate anion. Hence, this work demonstrates a very fast and inexpensive manner for the selective detection of acetate anion for the first time in a chemodosimetric way at very low concentration (μM level) in the presence and/or absence of other anions.

Experimental Section

Reagents and Materials: 4-Chloro-2,6-diformylphenol was prepared according to the literature method.[33] Copper perchlorate hexahydrate and zinc perchlorate hexahydrate were purchased from Merck (India); 2-thiophene-ethylamine and [D$_6$]DMSO were purchased from Sigma–Aldrich. All other chemicals and solvents were of reagent grade and have been used as received without further purification.

Synthesis of the Ligand HL: A solution containing 4-chloro-2,6-diformylphenol (1 mmol, 0.189 g) and 2-thiophene ethylamine (2 mmol, 0.254 g) in acetonitrile (25 mL) was refluxed for 45 min. A wax-like yellow liquid was obtained upon evaporation and it was washed several times with ether. After the evaporation of ether the sample purity was monitored by TLC (yield 90%, M_r = 402.97 g mol^{-1}). UV/Vis (acetonitrile, 900–200 nm): λ = 237 (ε = 105864 $M^{-1}cm^{-1}$), 350 (ε = 15413 $M^{-1}cm^{-1}$), and 452 (ε = 2970 $M^{-1}cm^{-1}$) nm. ^{1}H NMR (300 MHz, [D$_6$]DMSO, 25 °C, TMS): δ = 8.53 (s, 2 H); 7.67 (s, 2 H); 7.31 (dd, J = 5.1 and J = 1.2 Hz, 2 H); 6.89–6.94 (m, 4 H); 3.83 (t, J = 6.6 Hz, 4 H); 3.16 (t, J = 6.6 Hz, 4 H) ppm. FTIR (KBr pellet): $\tilde{\nu}$ = 3073.4 (m), 2920 (m), 2851 (m), 1641.9 (s), 1586 (m), 1437 (s), 1373 (m), 1301 (s), 1254 (s), 828 (m), 696 (s) cm^{-1}.

Synthesis of $[Cu_4(L)_2(OAc)_4(O)]$ (1): Copper(II) acetate monohydrate (0.399 g, 2 mmol) dissolved in acetonitrile (15 mL) was added dropwise to a solution of HL (0.382 g, 1 mmol) in acetonitrile (15 mL). The resulting solution was stirred for 2 h and a deep green solution was obtained. After keeping the solution for 2 d block-shaped green crystals suitable for X-ray structural determination were separated out, yield 84%; M_r = 1310.20 g mol^{-1}. UV/Vis (DMSO, 900–200 nm): λ = 378 (LMCT, ε = 11123 $M^{-1}cm^{-1}$) and 670 (d–d transition, ε = 370 $M^{-1}cm^{-1}$) nm. $C_{48}H_{48}Cl_2Cu_4N_4O_{11}S_4$ (1310.26): calcd. C 43.96, H 3.69, N 4.27; found C 43.85, H 3.61, N 4.22. FTIR (KBr pallet): $\tilde{\nu}$ = 3068.9 (s), 2918.70 (s), 2869.8 (s), 1640 (s), 1621 (s), 1603.6 (s), 1599 (s), 1557 (s), 1454.4 (s), 1392.0 (s), 1333.54 (s), 1240.4 (m), 847.43 (m), 691.83 (s) cm^{-1}.

Synthesis of $[Cu_2(L')_2(ClO_4)_2]$ (2): Copper(II) perchlorate (0.399 g, 1 mmol) dissolved in acetonitrile (15 mL) was added dropwise to a solution of HL (0.403 g, 1 mmol) in acetonitrile (15 mL). The resulting solution was stirred for 30–40 min and then kept at rest. After a week deep green block-shaped crystals suitable for X-ray structural determination were separated out (yield 81%, M_r = 911.48 g mol^{-1}). UV/Vis (DMSO, 900–200 nm): λ = 385 (LMCT, ε = 14926 $M^{-1}cm^{-1}$) and 728 (d–d transition, ε = 342 $M^{-1}cm^{-1}$) nm. IR (KBr pellet): $\tilde{\nu}$ = 3110.4.2 (m) 2882.3 (s), 2346.36 (s), 1646.02

(s), 1623.26 (s), 1555.86 (s), 1405.84 (s), 1330 (s), 1066.97 (s), 760.30 (s), 695.83 (s) 617.81 (s) cm^{-1}. $C_{28}H_{22}Cl_4Cu_2N_2O_{12}S_2$ (911.51): calcd. C 36.86, H 2.43, N 3.07; found C 36.73, H 2.37, N 2.99.

Synthesis of [$Cu_4(L)_2(OAc)_4(O)$] (3): Copper(II) perchlorate (0.399 g, 1 mmol) dissolved in acetonitrile (15 mL) was added dropwise to a solution of HL (0.403 g, 1 mmol) in acetonitrile (15 mL). The resulting solution was stirred for 30–40 min. Acetate monohydrate (0.198 g, 2 mmol) dissolved in a minimum quantity of 1:4 water/acetonitrile (10 mL) was added dropwise to this solution and stirred again for another 40–50 min. The bluish green solution turned into a light green one. After a couple of days rhombus-shaped green crystals suitable for X-ray data collection were obtained from that solution (yield 79%, M_r = 1310.20 g mol^{-1}). UV/Vis (DMSO, 900–200 nm): λ = 373 (LMCT, ε = 9250 M^{-1} cm^{-1}) and 675 (d–d transition, ε = 300 M^{-1} cm^{-1}) nm. IR (KBr pellet): $\tilde{\nu}$ = 3045.6 (m), 2921.37 (s), 2851.07 (m), 1623.6 (s), 1618.6 (s), 1576.5 (s), 1551.5 (s), 1447.75 (s), 1388.4 (s), 1335.8 (s), 696.3 (s), 626.7 (m) cm^{-1}. $C_{48}H_{48}Cl_2Cu_4N_2O_{11}S_4$ (1282.24): calcd. C 43.96, H 3.69, N 4.27; found C 43.87, H 3.63, N 4.24.

***CAUTION:** Perchlorate salts with organic ligands are potentially explosive. Only a small amount of material should be prepared and handled with caution.*

Preparation of Test Solutions for Fluorescence Titration: The initial stock solution of chemodosimeter **2** was prepared in acetonitrile by mixing HL (1×10^{-4} M) and copper perchlorate (1×10^{-4} M) in a 1:1 volume ratio that results in a solution of approximately 0.5×10^{-4} M. The increase in absorbance at 410 nm of the resulting solution was tuned with time in order to assure the complete formation of chemodosimeter **2**. After the formation of **2** was confirmed, the solution was further diluted to 5×10^{-6} M in CH_3CN and this solution was used as a final stock for fluorescence titration. The final stock solutions of various anions (as tetrabutylammonium salt) were prepared at 5×10^{-4} M by dilution from an initial stock of 0.1 M each. In each individual titration experiment, 2-mL test solutions contained 1 mL of stock chemodosimeter (5×10^{-6} M), 1 mL of acetonitrile, and 4–40 µL of the corresponding anion from a 5×10^{-4} M stock solution. The resulting solution was shaken well and incubated for 10 min at room temperature before the titration experiment started.

X-ray Data Collections and Structure Determinations: Diffraction data for compounds **1**, **2**, and **3** were collected with a Bruker Smart Apex diffractometer equipped with CCD. All the experiments were performed at room temperature with Mo-K_α radiation (λ = 0.71073 Å). Cell refinement, indexing, and scaling of the data set were carried out using Bruker Smart Apex and Bruker Saint packages.[34] The structures were solved by direct methods and subsequent Fourier analyses and refined by the full-matrix least-squares method based on F^2 with all observed reflections. The contribution from H atoms at calculated positions generated by the program SHELXL[35] was introduced in the final cycles of refinement. The independent thiophene rings of compounds **2** and **3** were found disordered showing two coplanar positions rotated by 180°. The refined occupancies in the former are 0.62(2)/0.38(2), while in **3** the atoms close to the *ipso* carbon in the thiophene ring were refined as mixed S/C species with 0.522(8)/0.478(8) occupancy and vice-versa. The sulfur atoms of **1** display a large thermal ellipsoid likely indicating a disorder but only one ring was refined with a mixed S/C species of a 0.657(18)/0.343(18) population. Crystallographic data and details of refinements are reported in Table S1. All the calculations were performed using the WinGX System, v. 1.80.05.[36] Pertinent crystallographic data and refinement details are summarized in Table 5.

CCDC-979728 (for **1**), -979729 (for **2**), and -979730 (for **3**) contain the supplementary crystallographic data for this paper. These data can be obtained free of charge from The Cambridge Crystallographic Data Centre via www.ccdc.cam.ac.uk/data_request/cif.

Supporting Information (see footnote on the first page of this article): FTIR spectra and electronic spectra.

Table 5. Crystallographic data and details of refinements for complexes **1**, **2**, and **3**.

	1	**2**	**3**
Empirical formula	$C_{48}H_{48}Cl_2Cu_4N_4O_{11}S_4$	$C_{28}H_{22}Cl_4Cu_2N_2O_{12}S_2$	$C_{48}H_{48}Cl_2Cu_4N_4O_{11}S_4$
M_r [g mol^{-1}]	1310.20	911.48	1310.20
Crystal system	triclinic	orthorhombic	tetragonal
Space group	$P\bar{1}$	$Pbca$	$I4_1/a$
a [Å]	12.7887(7)	12.302(5)	15.0647(14)
b [Å]	14.4793(8)	13.388(5)	
c [Å]	16.7982(10)	20.513(5)	24.013(2)
α [°]	106.456(2)	90	90
β [°]	98.485(2)	90	90
γ [°]	98.593(2)	90	90
V [Å^3]	2889.9(3)	3378(2)	5449.6(9)
Z	2	4	4
$D_{calcd.}$ [g cm^{-3}]	1.506	1.792	1.597
μ [mm^{-1}]	1.746	1.764	1.851
$F(000)$	1332	1832	2664
Total data	29449	32715	25971
Unique data	8911	2778	1910
R_{int}	0.0463	0.0341	0.0620
Reflections $I > 2\sigma(I)$	6724	2367	1500
Parameters	659	227	168
Goodness-of-fit	1.039	1.100	1.043
R_1	0.0739	0.0476	0.0349
wR_2 [$I > 2\sigma(I)$][a]	0.2025	0.1264	0.0863
Residuals [e Å^{-3}]	0.909, –0.693	0.953, –0.378	0.357, –0.279

[a] $R_1 = \Sigma \| F_o| - |F_c\| / \Sigma |F_o|$, $wR_2 = \{\Sigma[w(F_o^2 - F_c^2)^2] / \Sigma[w(F_o^2)^2]\}^{1/2}$.

Acknowledgments

The authors wish to thank the Council of Scientific and Industrial Research (CSIR), New Delhi [project number 01(2464)/11/EMR-II, dated 16-05-2011, grant to D. D. and project number 09/028(0766)/2010-EMR-I, dated 22/02/2010, grant to S. D.] for financial support. The Department of Science and Technology (DST), New Delhi is thanked for providing the single-crystal diffractometer facility at the Department of Chemistry, University of Calcutta, through the DST-FIST program.

---

[1] E. Duncan, P. J. A. Kleinman, A. N. Sharpley, in: *eLS*, John Wiley & Sons, Hoboken, **2012**.
[2] B. J. Calnan, B. Tidor, S. Biancalana, D. Hudson, A. D. Frankel, *Science* **1991**, *252*, 1167–1171.
[3] J. L. Sessler, P. I. Sansom, V. Král, D. O'Connor, B. L. Iverson, *J. Am. Chem. Soc.* **1996**, *118*, 12322–12330.
[4] J. Scheele, P. Timmerman, D. N. Reinhoudt, *Chem. Commun.* **1998**, 2613–2614.
[5] a) P. A. Gale, S. E. Garcia-Garrido, J. Garric, *Chem. Soc. Rev.* **2008**, *37*, 151–190; b) P. D. Beer, P. A. Gale, *Angew. Chem. Int. Ed.* **2001**, *40*, 486–516; *Angew. Chem.* **2001**, *113*, 502.
[6] R. M. Duke, E. B. Veale, F. M. Pfeffer, P. E. Kruger, T. Gunnlaugsson, *Chem. Soc. Rev.* **2010**, *39*, 3936–3953.
[7] C. R. Bondy, S. J. Loeb, *Coord. Chem. Rev.* **2003**, *240*, 77–99.
[8] T. Gunnlaugsson, M. Glynn, G. M. Tocci, P. E. Kruger, F. M. Pfeffer, *Coord. Chem. Rev.* **2006**, *250*, 3094–3117.
[9] J. L. Sessler, P. A. Gale, W. S. Cho, *Anion Receptor Chemistry*, The Royal Society of Chemistry, Cambridge, UK, **2006**, chapter 5.
[10] V. Amendola, D. Esteban-Gómez, L. Fabbrizzi, M. Licchelli, *Acc. Chem. Res.* **2006**, *39*, 343–353.
[11] B. T. Nguyen, E. V. Anslyn, *Coord. Chem. Rev.* **2006**, *250*, 3118–3127.
[12] M. Y. Chae, A. W. Czarnik, *J. Am. Chem. Soc.* **1992**, *114*, 9704–9705.
[13] Z. Xu, X. Chen, H. N. Kim, J. Yoon, *Chem. Soc. Rev.* **2010**, *39*, 127–137.
[14] R. Martínez-Máñez, F. Sancenón, *Chem. Rev.* **2003**, *103*, 4419–4476.
[15] L. Gai, H. Chen, B. Zou, H. Lu, G. Lai, Z. Li, Z. Shen, *Chem. Commun.* **2012**, *48*, 10721–10723.
[16] D.-G. Cho, J. L. Sessler, *Chem. Soc. Rev.* **2009**, *38*, 1647–1662.
[17] K. Kaur, R. Saini, A. Kumar, V. Luxami, N. Kaur, P. Singh, S. Kumar, *Coord. Chem. Rev.* **2012**, *256*, 1992–2028.
[18] Y. Yang, Q. Zhao, W. Feng, F. Li, *Chem. Rev.* **2013**, *113*, 192–270.
[19] M. Emrullahoglu, M. Ucuncu, E. Karakus, *Chem. Commun.* **2013**, *49*, 7836–7838.
[20] T.-Y. Ho, M. I. Scranton, G. T. Taylor, R. Varela, R. C. Thunell, F. Muller-Karger, *Limnol. Oceanogr.* **2002**, *47*, 1119–1128.
[21] J. March, *Advanced Organic Chemistry: Reactions, Mechanisms, and Structure*, 4th ed., John Wiley & Sons, New York, **1992**.
[22] J. Xie, Y. Zheng, J. Y. Ying, *Chem. Commun.* **2010**, *46*, 961–963.
[23] A. P. de Silva, H. Q. N. Gunaratne, T. Gunnlaugsson, A. J. M. Huxley, C. P. McCoy, J. T. Rademacher, T. E. Rice, *Chem. Rev.* **1997**, *97*, 1515–1566.
[24] T. Kundu, A. Dutta Chowdhury, D. De, S. M. Mobin, V. G. Puranik, A. Datta, G. K. Lahiri, *Dalton Trans.* **2012**, *41*, 4484–4496.
[25] N. DiCesare, M. R. Pinto, K. S. Schanze, J. R. Lakowicz, *Langmuir* **2002**, *18*, 7785–7787.
[26] A. N. Swinburne, M. J. Paterson, A. Beeby, J. W. Steed, *Org. Biomol. Chem.* **2010**, *8*, 1010–1016.
[27] G. De Santis, L. Fabbrizzi, M. Licchelli, A. Poggi, A. Taglietti, *Angew. Chem. Int. Ed.* **2003**, *35*, 202–204; *Angew. Chem.* **2003**, *115*, 212.
[28] D. Das, A. Guha, S. Das, P. Chakraborty, T. K. Mondal, S. Goswami, E. Zangrando, *Inorg. Chem. Commun.* **2012**, *23*, 113–116.
[29] S. Jana, S. Dalapati, N. Guchhait, *Photochem. Photobiol. Sci.* **2013**, *12*, 1636–1648.
[30] H. C. Hung, Y. Y. Chang, L. Luo, C. H. Hung, E. W. G. Diau, W. S. Chung, *Photochem. & Photobiol. Sci.* **2014**, DOI: 10.1039/C3PP50175B.
[31] B. Roy, T. Noguchi, D. Yoshihara, Y. Tsuchiya, A. Dawna, S. Shinkai, *Org. Biomol. Chem.* **2014**, *12*, 561–565.
[32] J. Xie, Y. Zheng, J. Y. Ying, *Chem. Commun.* **2010**, *46*, 961–963.
[33] R. R. Gagne, C. L. Spiro, T. J. Smith, C. A. Hamann, W. R. Thies, A. D. Shiemke, *J. Am. Chem. Soc.* **1981**, *103*, 4073–4081.
[34] *SMART*, *SAINT*, Software Reference Manual, Bruker AXS Inc., Madison, WI, **2000**.
[35] *SHELXL-97*, *Programs for Crystal Structure Analysis*, rel. 97–2, G. M. Sheldrick, University of Göttingen, Germany, **1998**.
[36] L. J. Farrugia, *J. Appl. Crystallogr.* **1999**, *32*, 837–838.

Received: June 12, 2014